DALTON
FULL PAPER

Unsymmetrically substituted pyrazolates: nickel(II) complexes of a novel dinucleating ligand providing both N- and S-rich co-ordination spheres ‡

Matthias Konrad, Franc Meyer,*,† Katja Heinze and Laszlo Zsolnai

Anorganisch-Chemisches Institut der Universität Heidelberg, Im Neuenheimer Feld 270, D-69120 Heidelberg, Germany

An unsymmetric pyrazolate ligand with different chelating side arms in the 3 and 5 positions of the heterocycle {3-[$(EtSCH_2CH_2)_2NCH_2$]-5-[$(Et_2NCH_2CH_2)_2NCH_2$]$C_3N_2H_2$ (HL^1)} and its symmetrical analogue {3,5-[$(EtSCH_2CH_2)_2NCH_2]_2C_3N_2H_2$($HL^2$)} have been prepared. Upon reaction with $NiCl_2·6H_2O$ they afforded dinuclear complexes $[Ni_2L^1Cl_3]$ **2** and $[Ni_2L^2Cl_3]$ **1** that contain both a bridging pyrazolate and a bridging chlorine atom. While all nickel(II) ions within the N_2S_2 compartments of the primary ligands are six-co-ordinate, one of the amino side arms of L^1 in the former complex is non-co-ordinating, leaving the respective nickel centre in a square-pyramidal environment. This dangling arm is co-ordinated to the metal ion upon treatment of **2** with $NaBPh_4$ due to substitution of the terminal chlorine atom to form $[Ni_2L^1Cl_2][BPh_4]$ **3**. All new complexes were characterised by means of X-ray crystallography; **2** and **3** represent rare examples of dinuclear complexes exhibiting various kinds of asymmetry. The electrochemical and magnetic properties of the complexes are reported.

The current interest in bi- and multi-metallic transition-metal complexes first of all arises from the fact that many active centres of metalloenzymes contain several co-operating metal ions in close proximity.[1] The individual metal centres often play specific and different roles in the functioning of the enzyme and consequently most of the oligonuclear metallobiosites have turned out to be of asymmetric character.[2] However, whereas many examples of bimetallic co-ordination compounds derived from symmetric dinucleating ligands have been described,[3] multidentate ligand systems with differentiated co-ordination spheres, which necessarily give asymmetric dinuclear complexes, have remained rare.[4] Hence the design and synthesis of new unsymmetric dinucleating ligand matrices providing distinct donor sets for each metal centre is highly desirable in order to obtain model complexes for the different types of asymmetry possibly present in such dinuclear cores, *i.e.* donor atom, co-ordination number or geometric asymmetry of either homo- or hetero-dinuclear character.[4c,5] Apart from the bioinorganic motivation, distinct reactivity patterns of unsymmetric dinuclear entities towards substrate molecules can be expected, *e.g.* resulting from the co-operative effects of both hard and soft metal centres located in close proximity.[6]

The vast majority of the unsymmetric dinucleating ligands hitherto reported is based on a bridging phenoxo- or alkoxo-group.[4,5] Although the ability of diazine heterocycles like pyrazolates to span two metal centres in a bridging fashion is well established,[7] relatively few studies of dinuclear complexes of pyrazolate ligands providing additional chelating substituents have been performed.[8–14] In particular, only one pyrazolate ligand with different substituents in the 3 and 5 positions of the heterocycle has been described, in which however the differentiation between the two co-ordination spheres is marginal as it consists of only one additional methyl group attached to a pyridyl side arm.[12]

In recent work we described the synthesis of dinuclear complexes derived from a series of pyrazolate-based ligands with pendant polyamino side arms[13a] and demonstrated the possibility selectively to tune the range of accessible metal–metal separations in these systems by variation of the side arm chain length.[13b] The present contribution deals with a new synthetic strategy to allow access to dinucleating pyrazolate-based ligands with chemically non-equivalent environments for the two metal centres. Emphasis is placed on a distinction of the two co-ordination compartments with regard to the hardness of the donor sites, *i.e.* one donor set is composed of only nitrogen donors with the other donor set comprised of mixed sulfur–nitrogen atoms, and on an asymmetry regarding the co-ordination number of the two metal ions. Dinuclear nickel(II) complexes are prepared and characterised structurally in order to probe the co-ordination potential of the new ligand system. Furthermore a related symmetric system is synthesized and studied for comparison.

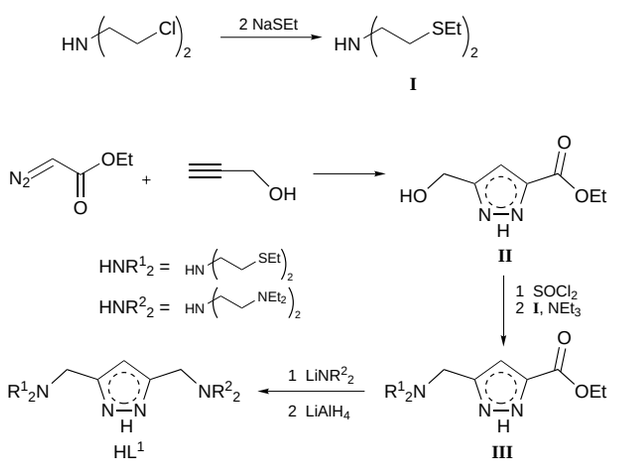

Scheme 1

Results and Discussion

The synthesis of the unsymmetric pyrazolate-based ligand HL^1 carrying pendant side arms with different donor sets in the 3 and 5 positions of the heterocycle is accomplished as outlined in Scheme 1. Cycloaddition of ethyl diazoacetate and prop-2-ynyl alcohol yields the unsymmetrically substituted pyrazole derivative **II**.[15] Conversion of its hydroxymethyl group into a

† E-Mail: franc@sun0.urz.uni-heidelberg.de
‡ *Non-SI unit employed*: $\mu_B = 9.27 \times 10^{-24}$ J T^{-1}.

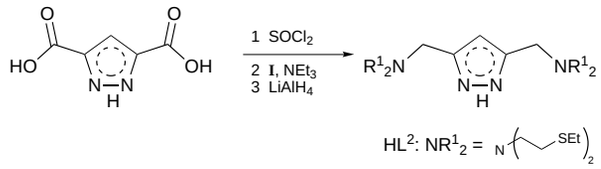

Scheme 2

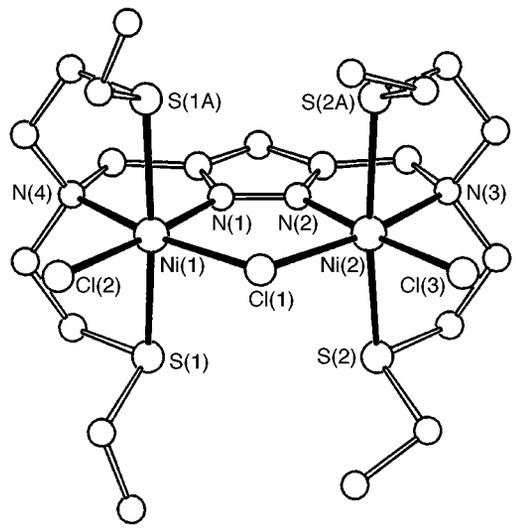

Fig. 1 View of the molecular structure of complex **1**. For clarity all hydrogen atoms have been omitted

chloromethyl function by means of $SOCl_2$ followed by treatment with the appropriate secondary amine **I** [prepared from bis(2-chloroethyl)amine as shown in Scheme 1] in the presence of triethylamine attaches the first donor side arm **III**. Subsequent reaction with the lithiated amine NR^2_2H and reduction of the resulting amide using $LiAlH_4$ affords the unsymmetric potential ligand HL^1 which provides both an N_4 and an N_2S_2 co-ordination compartment. It should be noted that beyond the preparation of HL^1 the reaction sequence described here opens up a more general access to various unsymmetric pyrazolate-based ligand systems with variable chelating side arms.

The corresponding symmetric $(N_2S_2)_2$ dinucleating ligand HL^2 was synthesized following a strategy described previously for the related $(N_4)_2$ analogue,[9d,13a] Scheme 2.

Synthesis and structural characterisation of nickel(II) complexes

In order to gain some basic knowledge about the general co-ordination mode of the N_2S_2 donor compartment of these novel pyrazolate ligands, we first studied a dinickel(II) complex of the symmetric species HL^2. The green neutral complex $[Ni_2L^2Cl_3]$ **1** is produced when the ligand HL^2 is first deprotonated by means of LiBu and subsequently treated with 2 equivalents of $NiCl_2{\cdot}6H_2O$. Complex **1** shows good solubility in tetrahydrofuran (thf) or CH_2Cl_2 and proved to be stable in air over prolonged periods. Single crystals suitable for a crystallographic analysis were obtained by vapour diffusion of Et_2O into a CH_2Cl_2 solution of the product. The molecular structure of **1** is depicted in Fig. 1 and selected distances and angles are given in Table 1.

The structure reveals a dinuclear arrangement of two nickel ions spanned by both the pyrazolate of L^2 and a bridging chlorine atom. Each nickel centre is found in an $N_2S_2Cl_2$ environment, slightly distorted from octahedral due to the limited dimensions of the chelate rings of the primary ligand side arms [*e.g.* S(1)–Ni(1)–S(1A) 166.59(8), [S(2)–Ni(2)–S(2A) 167.69(7)°]. The pyrazolate heterocycle as well as the nickel ions and the donor atoms N(3), N(4), Cl(1), Cl(2) and Cl(3) lie within a mirror plane of the dinuclear molecule that has crystallographically imposed C_s symmetry.

Table 1 Selected distances (Å) and angles (°) for complex **1**

Ni(1)–N(1)	1.975(6)	Ni(2)–N(3)	2.214(6)
Ni(1)–N(4)	2.195(5)	Ni(2)–Cl(3)	2.350(2)
Ni(1)–Cl(2)	2.367(2)	Ni(2)–Cl(1)	2.422(2)
Ni(1)–Cl(1)	2.430(2)	Ni(2)–S(2)	2.4886(14)
Ni(1)–S(1)	2.475(2)	Ni(2)–S(2A)	2.489(2)
Ni(1)–S(1A)	2.475(2)	Ni(1)···Ni(2)	3.823
Ni(2)–N(2)	1.991(5)		
N(1)–Ni(1)–N(4)	78.1(2)	N(2)–Ni(2)–Cl(3)	174.4(2)
N(1)–Ni(1)–Cl(2)	174.7(2)	N(3)–Ni(2)–Cl(3)	96.9(2)
N(4)–Ni(1)–Cl(2)	96.5(2)	N(2)–Ni(2)–Cl(1)	89.3(2)
N(1)–Ni(1)–Cl(1)	89.3(2)	N(3)–Ni(2)–Cl(1)	166.7(2)
N(4)–Ni(1)–Cl(1)	167.4(2)	Cl(3)–Ni(2)–Cl(1)	96.33(7)
Cl(2)–Ni(1)–Cl(1)	96.07(7)	N(2)–Ni(2)–S(2)	87.61(4)
N(1)–Ni(1)–S(1)	86.06(4)	N(3)–Ni(2)–S(2)	83.95(3)
N(4)–Ni(1)–S(1)	83.89(4)	Cl(3)–Ni(2)–S(2)	91.82(4)
Cl(2)–Ni(1)–S(1)	93.42(4)	Cl(1)–Ni(2)–S(2)	95.64(3)
Cl(1)–Ni(1)–S(1)	95.36(4)	N(2)–Ni(2)–S(2A)	87.61(4)
N(1)–Ni(1)–S(1A)	86.06(4)	N(3)–Ni(2)–S(2A)	83.95(3)
N(4)–Ni(1)–S(1A)	83.89(4)	Cl(3)–Ni(2)–S(2A)	91.82(4)
Cl(2)–Ni(1)–S(1A)	93.42(4)	Cl(1)–Ni(2)–S(2A)	95.64(3)
Cl(1)–Ni(1)–S(1A)	95.36(4)	S(2)–Ni(2)–S(2A)	167.69(7)
S(1)–Ni(1)–S(1A)	166.59(8)	Ni(1)–Cl(1)–Ni(2)	103.99(7)
N(2)–Ni(2)–N(3)	77.4(2)		

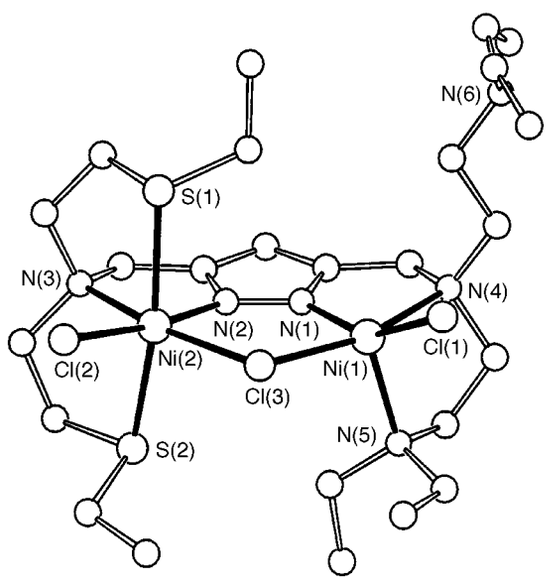

Fig. 2 View of the molecular structure of complex **2**. Details as in Fig. 1

Similar to the co-ordination behaviour of mononucleating tripodal tetradentate NS_3 ligands,[16] each co-ordination compartment of L^2 obviously allows for six-co-ordination of the metal centres, as long as the sulfur atoms bear small substituents like the present ethyl groups. In contrast, complexes containing a tripodal tetradentate NN_3 donor set are known to remain five-co-ordinate in the case of tertiary pendant nitrogen atoms. This is also true for the dinuclear nickel complexes of the unsymmetrical ligand HL^1 studied here. Treatment of the deprotonated potential ligand with 2 equivalents of $NiCl_2{\cdot}6H_2O$ affords the green neutral complex $[Ni_2L^1Cl_3]$ **2**, which crystallises upon vapour diffusion of Et_2O into a thf solution of the product. A view of the molecular structure of **2** is depicted in Fig. 2; selected distances and angles are listed in Table 2. As expected, **2** consists of a dinickel framework with both a bridging pyrazolate and a bridging chlorine atom. While Ni(2) is located in a distorted octahedral co-ordination environment that is essentially identical to those observed in **1**, Ni(1) is only five-co-ordinate, leaving one dangling side arm of the primary ligand non-co-ordinating. The co-ordination geometry around Ni(1) appears to be distorted square planar with N(5) in the

Table 2 Selected distances (Å) and angles (°) for complex **2**

Ni(1)–N(1)	1.952(3)	Ni(2)–N(3)	2.166(3)
Ni(1)–N(5)	2.089(4)	Ni(2)–Cl(2)	2.3518(12)
Ni(1)–N(4)	2.234(4)	Ni(2)–Cl(3)	2.4210(11)
Ni(1)–Cl(1)	2.2828(12)	Ni(2)–S(2)	2.4462(13)
Ni(1)–Cl(3)	2.3921(12)	Ni(2)–S(1)	2.5054(13)
Ni(2)–N(2)	1.981(3)	Ni(1) · · · Ni(2)	3.823
N(1)–Ni(1)–N(5)	100.71(14)	N(2)–Ni(2)–Cl(3)	87.78(10)
N(1)–Ni(1)–N(4)	78.07(14)	N(3)–Ni(2)–Cl(3)	166.59(10)
N(5)–Ni(1)–N(4)	86.67(14)	Cl(2)–Ni(2)–Cl(3)	96.33(4)
N(1)–Ni(1)–Cl(1)	152.32(11)	N(2)–Ni(2)–S(2)	88.43(10)
N(5)–Ni(1)–Cl(1)	105.48(10)	N(3)–Ni(2)–S(2)	83.70(9)
N(4)–Ni(1)–Cl(1)	94.51(10)	Cl(2)–Ni(2)–S(2)	96.51(5)
N(1)–Ni(1)–Cl(3)	88.95(10)	Cl(3)–Ni(2)–S(2)	96.77(4)
N(5)–Ni(1)–Cl(3)	102.63(10)	N(2)–Ni(2)–S(1)	90.34(10)
N(4)–Ni(1)–Cl(3)	165.32(10)	N(3)–Ni(2)–S(1)	85.23(9)
Cl(1)–Ni(1)–Cl(3)	93.89(4)	Cl(2)–Ni(2)–S(1)	83.90(4)
N(2)–Ni(2)–N(3)	78.84(13)	Cl(3)–Ni(2)–S(1)	94.21(4)
N(2)–Ni(2)–Cl(2)	173.14(10)	S(2)–Ni(2)–S(1)	168.89(4)
N(3)–Ni(2)–Cl(2)	96.93(10)	Ni(1)–Cl(3)–Ni(2)	105.19(4)

Table 3 Selected distances (Å) and angles (°) for complex **3**

Ni(1)–N(1)	1.936(4)	Ni(2)–N(3)	2.185(4)
Ni(1)–N(5)	2.125(4)	Ni(2)–Cl(2)	2.3242(13)
Ni(1)–N(6)	2.145(4)	Ni(2)–S(2)	2.4756(14)
Ni(1)–N(4)	2.156(4)	Ni(2)–S(1)	2.5029(14)
Ni(1)–Cl(1)	2.3972(12)	Ni(2)–Cl(1)	2.5600(12)
Ni(2)–N(2)	1.986(4)	Ni(1) · · · Ni(2)	3.903
N(1)–Ni(1)–N(5)	102.2(2)	N(2)–Ni(2)–S(2)	88.85(12)
N(1)–Ni(1)–N(6)	102.4(2)	N(3)–Ni(2)–S(2)	84.20(14)
N(5)–Ni(1)–N(6)	150.6(2)	Cl(2)–Ni(2)–S(2)	91.13(5)
N(1)–Ni(1)–N(4)	80.6(2)	N(2)–Ni(2)–S(1)	88.75(12)
N(5)–Ni(1)–N(4)	84.08(14)	N(3)–Ni(2)–S(1)	84.49(13)
N(6)–Ni(1)–N(4)	84.4(2)	Cl(2)–Ni(2)–S(1)	90.37(5)
N(1)–Ni(1)–Cl(1)	89.67(11)	S(2)–Ni(2)–S(1)	168.68(5)
N(5)–Ni(1)–Cl(1)	98.05(11)	N(2)–Ni(2)–Cl(1)	85.61(11)
N(6)–Ni(1)–Cl(1)	97.87(11)	N(3)–Ni(2)–Cl(1)	164.37(12)
N(4)–Ni(1)–Cl(1)	170.25(11)	Cl(2)–Ni(2)–Cl(1)	99.01(5)
N(2)–Ni(2)–N(3)	78.8(2)	S(2)–Ni(2)–Cl(1)	96.12(5)
N(2)–Ni(2)–Cl(2)	175.36(11)	S(1)–Ni(2)–Cl(1)	94.72(4)
N(3)–Ni(2)–Cl(2)	96.61(12)	Ni(1)–Cl(1)–Ni(2)	103.82(4)

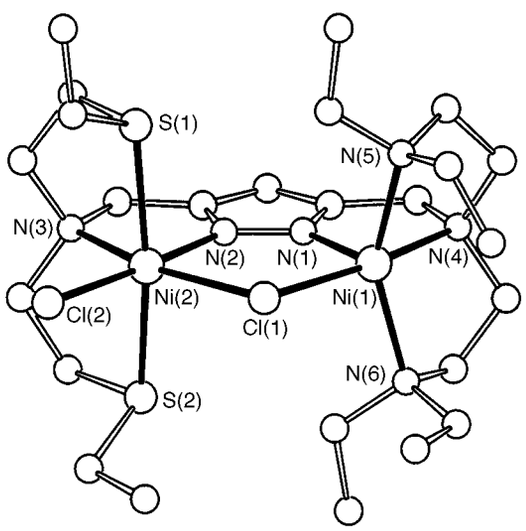

Fig. 3 Molecular structure of the cation of complex **3**. Details as in Fig. 1

apical position. Despite the inherent donor atom and co-ordination number asymmetry present in **2**, the Ni · · · Ni distances observed for **2** and the symmetric complex **1** are virtually identical [d(Ni · · · Ni) = 3.823 Å]. However, both the Ni–$N_{pyrazolate}$ and Ni–Cl_{bridge} bond lengths are slightly smaller for the five-co-ordinate metal ion {d[Ni(1)–N(1)] = 1.952(3); d[Ni(1)–Cl(3)] = 2.392(1) Å} compared to those for the six-co-ordinate metal ions {**2**: d[Ni(2)–N(2)] = 1.981(3); d[Ni(2)–Cl(3)] = 2.421(1) Å; **1**: d[Ni(1)–N(1)] = 1.975(6), d[Ni(2)–N(2)] = 1.991(5), d[Ni(1)–Cl(1)] = 2.430(2), d[Ni(2)–Cl(1)] = 2.422(2) Å}.

Reaction of complex **2** with 1 equivalent of $NaBPh_4$ induces co-ordination of the formerly dangling side arm to the Ni(1) centre due to substitution of the respective terminal chlorine atom. Single crystals of the resulting product $[Ni_2L^1Cl_2][BPh_4]$ **3** formed upon vapour diffusion of Et_2O into a thf solution of the complex. The molecular structure of the cation of **3** is shown in Fig. 3, selected distances and bond angles in Table 3. Atom Ni(1) is now found in a distorted trigonal-bipyramidal environment with the branching nitrogen atom N(4) and the bridging Cl(1) in axial positions. In accordance with the structural findings for a series of related symmetric dicobalt(II) complexes of pyrazolate-based polyamino ligands,[13a,b] co-ordination of all side arms of the tren-type NN_3 co-ordination subunit of L^1 pulls the two metal centres back and apart, thus causing a lengthening of the Ni · · · Ni separation when going from **2** to **3** [d(Ni · · · Ni) = 3.903 Å]. Interestingly, this leads to a significantly longer Ni(2)–Cl_{bridge} bond {d[Ni(2)–Cl(3)] = 2.421(1) in **2** *vs.* d[Ni(2)–Cl(1)] = 2.560(1) Å in **3**}, while the Ni(1)–Cl_{bridge} distance remains virtually unchanged {d[Ni(1)–Cl(3)] = 2.392(1) in **2** *vs.* d[Ni(1)–Cl(1)] = 2.397(1) in **3**}.

Complexes **2** and **3** thus represent dinuclear compounds that exhibit various kinds of asymmetry, examples of which have hitherto remained rare.

Spectroscopy and electrochemistry

The UV absorption spectrum of complex **1** displays three ligand-field transitions at 8730(ν_1), 15 550(ν_2) and 24 940(ν_3) cm^{-1} assigned to spin-allowed transitions from $^3A_{2g}$ to $^3T_{2g}$, $^3T_{1g}(F)$ and $^3T_{1g}(P)$, respectively, in accord with a d^8 ion in a near-octahedral co-ordination sphere.[17] The value $\Delta_{oct} \approx 8730$ cm^{-1} can be deduced from the ν_1 band, and a calculated Racah parameter $B \approx 880$ cm^{-1} results from consideration of an octahedral strong-field coupling scheme. Taking $15B = 15\,615$ cm^{-1} for the gaseous ion Ni^{2+} (^3P),[18] this leads to a nephelauxetic ratio β of 0.845.

In the case of the unsymmetrical complexes **2** and **3** similar UV absorptions characteristic for a d^8 ion with octahedral ligation[17] are observed at 9090, 14 290 and 24 630 cm^{-1} **2** and at 8840, 14 750 and 24 690 cm^{-1} **3**. However, an additional band at 23 470 cm^{-1} **2** and a shoulder at ≈23 800 cm^{-1} **3** appear, which are attributed to the presence of the second type of nickel(II) ions, *i.e.* the five-co-ordinate metal centres.[19]

All dinuclear complexes have been studied by cyclic voltammetry (CV) in the potential range 0.0 to +1.50 V *vs.* the saturated calomel electrode (SCE) in CH_2Cl_2 (Fig. 4). Complex **1** shows a reversible oxidation wave at $E_{\frac{1}{2}} = +0.87$ V followed by a second oxidation with $E_p^{ox} = +1.26$ V, these processes presumably corresponding to the sequential formation of $Ni^{III}Ni^{II}$ and $Ni^{III}Ni^{III}$ species, respectively. While the second oxidation wave at the more positive potential appears to be irreversible at low scan rates (50 mV s^{-1}), it changes its shape with increasing scan rates to become quasi-reversible and yield an $E_{\frac{1}{2}}$ value of +1.19 V. Attempts to oxidise **1** on a preparative scale are currently underway. The cyclic voltammogram of **2** displays an oxidation process at $E_p^{ox} = +1.13$ V (200 mV s^{-1}) with a shoulder at around +0.90 V, the main wave becoming quasi-reversible at higher scan rates to give $E_{\frac{1}{2}} = +1.06$ V. In contrast, **3** shows an oxidation wave with $E_p^{ox} = +0.93$ V (200 mV s^{-1}) that remains irreversible over the entire range of scan rates studied (50–1000 mV s^{-1}). Obviously the presence of the five-co-ordinate nickel ions in the unsymmetric complexes **2** and **3** prevents the reversible generation (on the time-scale of the CV experiment) of a mixed-valence $Ni^{III}Ni^{II}$ species.

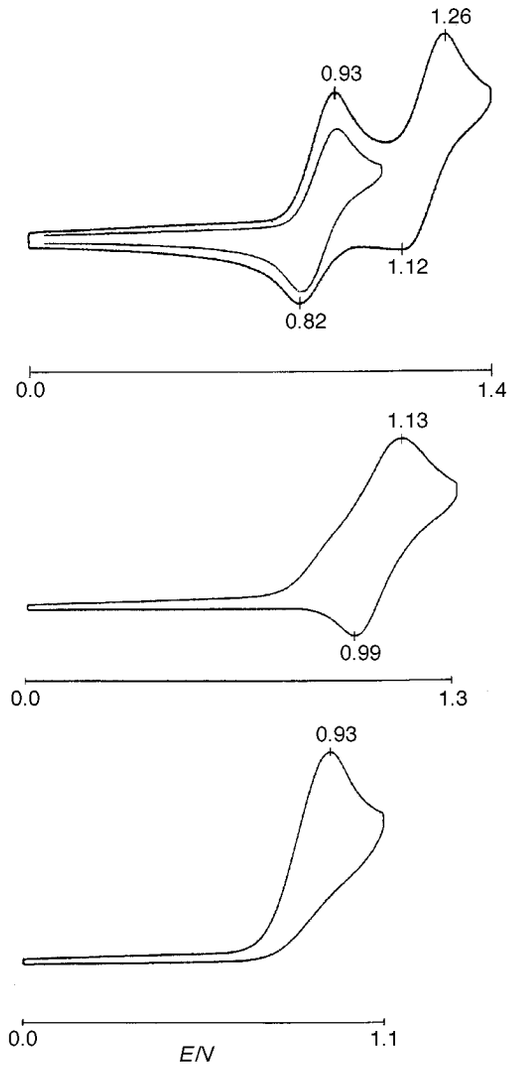

Fig. 4 Cyclic voltammograms of complex **1** (top), **2** (middle) and **3** (bottom) in CH_2Cl_2 containing 0.1 M $NBu^n_4PF_6$ at scan speed 200 mV s^{-1}

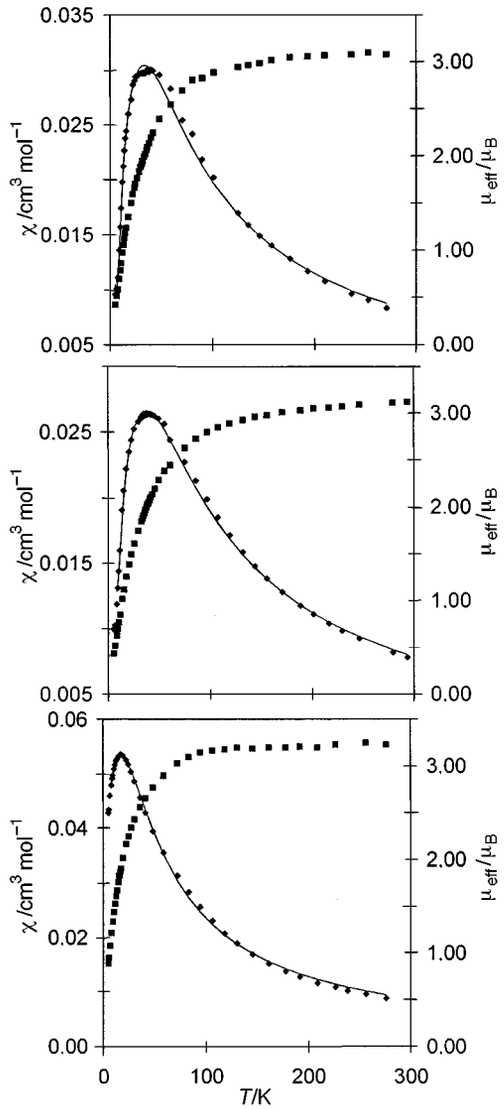

Fig. 5 Temperature dependence of the molar magnetic susceptibility (solid diamonds) and magnetic moment (solid squares) per nickel atom for complexes **1** (top), **2** (middle) and **3** (bottom). The line represents the calculated curve

Magnetic properties of the complexes

The magnetic properties of all new complexes have been studied in the solid state over the temperature range 5–290 K. The data obtained for the molar susceptibility and the effective magnetic moment are plotted in Fig. 5. The magnetic moment per nickel ion gradually decreases from 3.10 μ_B at 270 K (**1**), 3.12 μ_B at 293 K (**2**) and 3.25 μ_B at 275 K (**3**) to 0.43 μ_B at 4.7 K (**1**), 0.44 μ_B at 4.7 K (**2**) and 0.89 μ_B at 4.6 K (**3**), respectively, while the susceptibility curves exhibit broad maxima at around 35 (**1**), 40 (**2**) and 17 K (**3**), this behaviour being indicative of antiferromagnetic coupling between two nickel(II) centres in all cases. Fitting the experimental data by the theoretical expression for the isotropic spin Hamiltonian $H = -2J \cdot S_1 \cdot S_2$ (with $S_1 = S_2 = 1$) including a molar fraction p of uncoupled paramagnetic impurity [equation (1)][20] and neglecting the asymmetric character of the complexes yields the values listed in Table 4.§ In principle, powder measurements are not ideally suited for a thorough analysis of $S = 1$ dinuclear systems, however the intradimer exchange term J often proves to be the dominant term in the spin Hamiltonian[22,23] and accordingly the neglect of both a zero-field splitting parameter D and interdimer interactions $z'J'$ results in a good-quality fit in the present case (Fig. 5). The observed exchange interaction turns out to be only slightly smaller for **1** ($J = -12.0$ cm^{-1}) compared to **2** ($J = -13.1$ cm^{-1}), but significantly smaller for **3** ($J = -8.1$ cm^{-1}). Magnetostructural relationships for dinuclear nickel(II) systems are not yet as elaborate as the detailed correlations noted in copper(II) chemistry.[21] Furthermore, the fact that the complexes studied here differ by various structural parameters precludes the definitive deduction of any correlation between J and the structural data. However, it is interesting that a dependence of the antiferromagnetic exchange interaction on the metal–metal separation is perceptible. Thus the lengthening of the nickel–nickel distance in **3** compared to those in **1** and **2** is accompanied by a drastic decrease in the value of $-J$. The difference in J for **1** and **2** might be related to a more efficient orbital overlap for the five-co-ordinate metal ion caused by the

$$\chi = \chi_{dim}(1 - p) + 2\chi_{mono}p + 2N\alpha \qquad (1)$$

Table 4 Magnetic data for the complexes

Compound	J/cm^{-1}	g	p
1 $[Ni_2L^2Cl_3]$	−12.0	2.30	0.04
2 $[Ni_2L^1Cl_3]$	−13.1	2.27	0.03
3 $[Ni_2L^1Cl_2][BPh_4]$	−8.1	2.35	0.07

§ $N\alpha$ refers to the temperature-independent paramagnetism [100×10^{-6} cm^3 mol^{-1} per nickel(II) ion[21b]]; all other parameters have their usual meaning. $\chi_{dim} = (Ng^2\mu_B^2/kT)[2\exp(2J/kT) + 10\exp(6J/kT)]/[1 + 3\exp(2J/kT) + 5\exp(6J/kT)]$, $\chi_{mono} = 2Ng^2\mu_B^2/3kT$.

slightly shorter Ni–$N_{pyrazolate}$ and Ni–Cl_{bridge} bond lengths (see above). A substantial increase of the antiferromagnetic coupling that has been reported to occur when a six-co-ordinate species transforms to a five-co-ordinate square-pyramidal species in a series of doubly phenoxide-bridged dinickel(II) complexes is not observed in the present case.[23]

Conclusion

A synthetic strategy opening up access to unsymmetric dinucleating ligands containing a bridging pyrazolate moiety has been developed. The ligand HL^1 providing non-equivalent NN_3 and NNS_2 co-ordination compartments affords dinuclear nickel(II) complexes **2** and **3**, which exhibit both donor atom and co-ordination number asymmetry. The metal–metal distances are in the range 3.82–3.91 Å, thus stimulating further investigations with regard to achieving co-operative effects within complexes of this type. While the NNS_2 donor set allows for six-co-ordination of the respective metal centre (including both terminal and bridging chloride ligands), the nickel(II) ion ligated by the NN_3 subunit is restricted to five-co-ordination. The electrochemical oxidations of **2** and **3** are irreversible processes. In contrast, the symmetric complex **1** of the independently prepared $(NNS_2)_2$ ligand HL^2, which contains two six-co-ordinate nickel(II) ions, displays a reversible first oxidation wave, presumably generating the mixed-valent $Ni^{II}Ni^{III}$ species. Studies aimed at oxidising **1** on a preparative scale are in progress. While the magnetic properties of **1** and **2** differ only slightly, **3** shows a significantly decreased value for the antiferromagnetic exchange interaction, which is rationalised on the basis of its larger metal–metal separation. These results emphasise that distinct properties can be expected from subtle changes in ligation and from the introduction of asymmetry at dinuclear metal centres. Furthermore HL^1 as well as related unsymmetric dinucleating systems should prove promising candidates for a controlled synthesis of heterodinuclear complexes. Work in this regard is presently underway.

Experimental

All manipulations were carried out under an atmosphere of dry nitrogen by employing standard Schlenk techniques. Solvents were dried according to established procedures. The pyrazole derivative **II** was synthesized according to the reported method.[15] Microanalyses: Mikroanalytische Laboratorien des Organisch-Chemischen Instituts der Universität Heidelberg. IR spectra: Bruker IFS 66 FTIR. Proton and ^{13}C-{^1H} NMR spectra: Bruker AC 200 at 200.13 and 50.32 MHz, respectively; solvent signal as chemical shift reference ($CDCl_3$, δ_H 7.27, δ_C 77.0). FAB and EI mass spectra: Finnigan MAT 8230. UV/VIS/NIR spectra: Perkin-Elmer Lambda 19. Cyclic voltammetry: PAR equipment (potentiostat/galvanostat 273), on 0.1 M NBu_4PF_6–CH_2Cl_2. Potentials in V on glassy carbon electrode, referenced to the SCE at ambient temperature. Magnetic measurements: Bruker B-E 15 C8 Magnet, B-H 15 field controller, ER4111VT variable-temperature unit, Sartorius M 25 D-S micro balance.

Preparations

Bis[2-(ethylsulfanyl)ethyl]amine I. A solution of bis(2-chloroethyl)amine hydrochloride (8.8 g, 50.0 mmol) in ethanol (100 cm^3) was added to a solution of NaOH (6.0 g, 150.0 mmol) and ethanethiol (9.3 g, 150.0 mmol) in ethanol (150 cm^3) at 0 °C. The mixture was stirred for 2 h, filtered and the filtrate evaporated to dryness. The residue was taken up in Et_2O and filtered again. After evaporation of the solvent in vacuum, the *product* **I** (8.7 g, 90%) remained as a colourless semisolid (Found: C, 49.58; H, 9.79; N, 7.14. $C_8H_{19}NS_2$ requires C, 49.69; H, 9.90; N, 7.24%); $\delta_H(CDCl_3)$ 1.20 [6 H, t, *J*(HH) 7.4, CH_3], 2.49 [4 H, q, *J*(HH) 7.4 Hz, CH_2], and 2.60–2.80 (8 H, m, CH_2); $\delta_C(CDCl_3)$ 15.2 (CH_3), 26.1 (CH_2) 32.1 (CH_2) and 48.6 (CH_2); *m*/*z* 193 (M^+, 35), 118 ($M^+ - CH_2SEt$, 54) and 89 ($CH_2CH_2SEt^+$, 100%).

Ethyl 5-{*N*,*N*-bis[2-(ethylsulfanyl)ethyl]aminomethyl}pyrazole-3-carboxylate III. A solution of the pyrazole derivative **II**[15] (8.5 g, 50.0 mmol) in thionyl chloride (150 cm^3) was stirred for 3 h at 0 °C. After evaporation of the solvent in vacuum raw *ethyl 5-chloromethylpyrazole-3-carboxylate hydrochloride* (10.7 g, 95%) remained as a white solid; $\delta_H[(CD_3)_2SO]$ 1.28 [3 H, t, *J*(HH) 7.1, CH_3], 4.27 [2 H, q, *J*(HH) 7.1 Hz, CH_2], 4.76 (2 H, s, CH_2) and 6.82 (1 H, s, CH); $\delta_C(Me_2SO)$ 15.0 (CH_3), 37.7 (CH_2), 61.4 (CH_2Cl), 109.0 (pz C^4), 139.4, 145.9 (pz $C^{3/5}$) and 161.1 (C=O); *m*/*z* 188 ($M^+ - Cl$, 37), 153 ($M - 2$ Cl, 100) and 107 ($M - 2$ Cl − OEt, 28%). This compound (2.6 g, 10.0 mmol) was dissolved in thf (100 cm^3) and treated with a solution of **I** (1.9 g, 10.0 mmol) and triethylamine (5 cm^3) in thf (30 cm^3). The mixture was stirred for 2 h at room temperature. The triethylamine hydrochloride was then filtered off and the filtrate evaporated to dryness. The residue was taken up in Et_2O and filtered again. Evaporation of the solvent in vacuum afforded **III** (3.1 g, 89%) as a yellow oil (Found: C, 51.49; H, 7.76; N, 12.36. $C_{15}H_{27}N_3O_2S_2$ requires C, 52.14; H, 7.88; N, 12.16%); $\tilde{\nu}_{max}/cm^{-1}$ (film) 3136w (br), 2968–2927s, 1722vs, 1456s and 1227s; $\delta_H(CDCl_3)$ 1.26 [6 H, t, *J*(HH) 7.4, CH_3], 1.42 [3 H, t, *J*(HH) 7.2, CH_3], 2.54 [4 H, q, *J*(HH) 7.4, CH_2], 2.67–2.85 (8 H, m, CH_2), 3.81 (2 H, s, CH_2), 4.42 [2 H, q, *J*(HH) 7.2 Hz CH_2] and 6.70 (s, 1 H, CH); $\delta_C(CDCl_3)$ 14.7 (CH_3), 15.1 (CH_3), 26.6 (SCH_2), 30.1 (SCH_2), 49.9 (NCH_2), 54.1 (NCH_2), 61.4 (OCH_2), 107.1 (pz C^4), 142.8, 144.8 (pz $C^{3/5}$) and 162.4 (C=O); *m*/*z* 345 (M^+, 1), 270 ($M^+ - CH_2SEt$, 75) and 89 ($CH_2CH_2SEt^+$, 100%).

3-{*N*,*N*-Bis[2-(diethylamino)ethyl]aminomethyl}-5-{*N*,*N*-bis[2-(ethylsulfanyl)ethyl]aminomethyl}pyrazole (HL^1). A solution of LiBu (5.6 cm^3, 2.5 M) in hexane was added to a solution of *N*,*N*,*N*′,*N*′-tetraethyldiethylenetriamine (3.0 g, 13.9 mmol) in thf (50 cm^3) at −70 °C. This mixture was slowly added to a solution of compound **III** (2.4 g, 6.9 mmol) in thf (100 cm^3) at −70 °C. After warming to room temperature, the solution was left stirring overnight, then quenched with a saturated aqueous NH_4Cl solution and extracted several times with Et_2O. The combined organic phases were dried over $MgSO_4$ and filtered. After evaporation of the solvent in vacuum, 3-[N,N-*bis*[2-(*diethylamino*)*ethyl*]*carbamoyl*-5-{N,N-*bis*[2-(*ethylsulfanyl*)-*ethyl*]*aminoethyl*}*pyrazole* (3.0, 84%) remained as a yellow oil; $\delta_H(CDCl_3)$ 1.12 [12 H, t, *J*(HH) 7.1, CH_3], 1.27 [6 H, t, *J*(HH) 7.4 Hz, CH_3], 2.50–2.77 (24 H, m, CH_2), 3.51 (2 H, br t, $CONCH_2$), 3.75 (2 H, br s, $CONCH_2$), 3.80 (2 H, s, CH_2) and 6.68 (1 H, s, CH); $\delta_C(CDCl_3)$ 11.0 (CH_3), 14.6 (CH_3), 25.8 (CH_2), 29.1 (CH_2), 47.1 (CH_2), 49.7 (CH_2), 51.2 (CH_2), 53.1 (CH_2), 53.6 (CH_2), 101.9 (pz C^4), 143.4 and 148.5 (pz $C^{3/5}$), C=O not observed. A solution of this compound (3.0 g, 5.8 mmol) in thf (50 cm^3) was added dropwise to a suspension of $LiAlH_4$ (0.22 g, 5.8 mmol) in thf (100 cm^3) at room temperature. The mixture was left stirring overnight, then heated to reflux for 30 min, cooled to 0 °C and finally hydrolysed by the dropwise addition of water (2 cm^3). The precipitate was filtered off and washed several times with thf. The combined organic phases were dried over $MgSO_4$, filtered and evaporated to dryness to yield HL^1 (1.8 g, 62%) as a yellow oil (Found: C, 59.43; H, 10.29; N, 15.81. $C_{25}H_{52}N_6S_2$ requires C, 59.95; H, 10.47; N, 16.78%); $\tilde{\nu}_{max}/cm^{-1}$ (film) 2966–2811vs, 1453s, 1374s, 1294w, 1102s, 1069s and 801w; $\delta_H(CDCl_3)$ 1.08 [12 H, t, *J*(HH) 7.1, CH_3], 1.27 [6 H, t, *J*(HH) 7.4 Hz, CH_3], 2.50–2.76 (28 H, m, CH_2), 3.75 (2 H, s, CH_2), 3.78 (2 H, s, CH_2) and 5.99 (1 H, s, CH); $\delta_C(CDCl_3)$ 11.3 (CH_3), 15.1 (CH_3), 25.6 (SCH_2), 29.2 (SCH_2), 47.0–53.7 (NCH_2), 103.2 (pz C^4) and 142.8, 149.5 (pz $C^{3/5}$); *m*/*z* 501 ($M^+ + 1$, 100) and 414 ($M^+ - CH_2CH_2SEt$, 53%).

Table 5 Crystal data and refinement details for complexes **1**–**3**

	1	**2**	**3**
Formula	$C_{21}H_{41}Cl_3N_4Ni_2S_4{\cdot}CH_2Cl_2$	$C_{25}H_{51}Cl_3N_6Ni_2S_2$	$C_{49}H_{52}Cl_2N_6Ni_2S_2{\cdot}0.5C_4H_{10}O{\cdot}0.3C_4H_8O$
M_r	786.51	723.61	1058.60
Crystal size/mm	0.3 × 0.3 × 0.3	0.20 × 0.30 × 0.30	0.04 × 0.3 × 0.3
Crystal system	Orthorhombic	Monoclinic	Triclinic
Space group	*Pnma*	*C*2/*c*	$P\bar{1}$
a/Å	15.570(3)	42.712(9)	14.884(2)
b/Å	12.286(3)	10.960(2)	15.205(2)
c/Å	17.346(2)	14.176(2)	15.675(2)
α/°			70.82(1)
β/°		89.46(1)	65.93(1)
γ/°			62.85(1)
U/Å^3	3318.2(11)	6635.8	2837.5(6)
D_c/g cm^{-3}	1.574	1.449	1.239
Z	4	8	2
F(000)	1632	3056	1119
μ (Mo-K$_\alpha$) mm^{-1}	1.810	1.528	0.871
Scan mode	ω	ω	ω
hkl Ranges	−17 to 19, −8 to 15, −15 to 21	−6 to 51, ±13, ±17	0 to 18, 16 to 18, −17 to 19
2θ Range/°	3.5–52	3.8–51	3.8–52
Measured reflections	4306	6271	11 574
Observed reflections [$I > 2\sigma(I)$]	3429	6185	11 121
Refined parameters	222	357	654
Residual electron density e Å^{-3}	0.747, −1.313	0.536, −0.370	0.888, −0.403
*R*1	0.052	0.046	0.054
*wR*2	0.177	0.096	0.177
Goodness of fit	1.771	1.028	1.065

3,5-Bis{*N*,*N*-bis[2-(ethylsulfanyl)ethyl]aminoethyl}pyrazole (HL^2). Pyrazole-3,5-dicarboxylic acid monohydrate (1.7 g, 10.0 mmol) was converted into 3,5-bis(chloroformyl)pyrazole by the usual reaction with thionyl chloride (100 cm^3). This was taken up in thf (100 cm^3) and treated dropwise with a solution of compound **I** (3.9 g, 20.0 mmol) and triethylamine (5 cm^3) in thf (50 cm^3). After 2 h the triethylamine hydrochloride was filtered off and the filtrate evaporated to dryness. The residue was taken up in Et_2O and filtered again. After evaporation of the solvent in vacuum, 3,5-*bis*{N,N-*bis*[2-(*ethylsulfanyl*)*ethyl*]*carbamoyl*}-*pyrazole* (4.7 g, 93%) remained as a yellow oil; $\delta_H(CDCl_3)$ 1.25 (12 H, m, CH_3), 2.59 [8 H, q, *J*(HH) 7.4, SCH_2], 2.83 [8 H, t, *J*(HH) 7.3 Hz, SCH_2], 3.71 (4 H, br s, $CONCH_2$), 3.95 (4 H, br s, $CONCH_2$) and 7.07 (1 H, s, CH); $\delta_C(CDCl_3)$ 14.6 (CH_3), 25.8 (SCH_2), 28.6 (CH_2), 30.2 (CH_2), 47.7 (CH_2), 49.3 (CH_2), 109.2 (pz C^4), 141.1 (pz C$^{3/5}$) and 161.2 (C=O); *m*/*z* 507 (M^+ + 1, 20), 445 (M^+ − SEt, 23) and 89 (CH_2CH_2SEt, 100%). A solution of this compound (4.7 g, 9.3 mmol) in thf (50 cm^3) was added to a suspension of $LiAlH_4$ (0.7 g, 18.6 mmol) in thf (150 cm^3). The mixture was left stirring overnight, heated to reflux for 30 min, then cooled to 0 °C and finally hydrolysed by dropwise addition of water (4 cm^3). The precipitate was filtered off and washed several times with thf. The combined organic phases were dried over $MgSO_4$, filtered and evaporated to dryness to yield HL^2 (3.6 g, 80%) as a yellow oil (Found: C, 52.26; H, 9.03; N, 11.31. $C_{21}H_{42}N_4S_4$ requires C, 52.67; H, 8.84; N, 11.70%); $\tilde{\nu}_{max}$/cm^{-1} (film) 3191s, 2945–2823vs, 1466vs, 1369s, 1263s, 1105s, 993w and 783w; $\delta_H(CDCl_3)$ 1.24 [12 H, t, *J*(HH) 7.4, CH_3], 2.30 [8 H, q, *J*(HH) 7.4 Hz, SCH_2], 2.63–2.85 (16 H, m, CH_2), 3.69 (4 H, s, CH_2) and 6.03 (1 H, s, CH); $\delta_C(CDCl_3)$ 15.3 (CH_3), 26.6 (SCH_2), 30.1 (SCH_2), 54.2 (NCH_2) and 103.7 (pz C^4), pz C$^{3/5}$ not observed; *m*/*z* 479 (M^+ + 1, 6), 403 (M^+ − CH_2SEt, 22) and 89 ($CH_2CH_2SEt^+$, 100%).

[Ni$_2$L^{2}Cl$_3$] 1. A solution of LiBu (0.4 cm^3, 2.5 M) in hexane and a solution of $[Ni(H_2O)_6]Cl_2$ (0.48 g, 2.0 mmol) in ethanol (20 cm^3) were added stepwise to a solution of HL^2 (0.48 g, 1.0 mmol) in thf (50 cm^3). The green reaction mixture was evaporated to dryness and the resulting green powder (0.67 g, 85%) washed several times with small portions of ethanol. Vapour diffusion of Et_2O into a solution of the product in CH_2Cl_2 gave blue-green *crystals* of [Ni$_2$L^{2}Cl$_3$] **1** (0.33 g, 47%) (Found: C, 35.55; H, 5.95; N, 7.94. $C_{21}H_{41}Cl_3N_4Ni_2S_4$ requires C, 35.95; H, 5.89; N, 7.99%); $\tilde{\nu}_{max}$/cm^{-1} (KBr) 2960–2841vs, 1473s, 1457s, 1416s, 1266w, 1100s, 775w and 756w; *m*/*z* 664 (M^+ − Cl, 100) and 600 (M^+ − Cl − EtCl, 18%); λ_{max}/nm (ε/dm^3 mol^{-1} cm^{-1}) (CH_2Cl_2) 401 (131), 643 (27) and 1145 (49).

[Ni$_2$L^{1}Cl$_3$] 2. Starting from HL^1 (0.50 g, 1.0 mmol) the preparation was carried out analogously to that for **1** to yield the raw product (0.66 g, 91%). Vapour diffusion of Et_2O into a solution of the product in thf gave green *crystals* of [Ni$_2$L^{1}Cl$_3$] **2** (0.25 g, 35%) (Found: C, 40.23; H, 7.04; N, 11.17. $C_{25}H_{51}Cl_3N_6Ni_2S_2$ requires C, 41.50; H, 7.10; N, 11.61%); $\tilde{\nu}_{max}$/cm^{-1} (KBr) 2965–2844vs, 1471s, 1463s, 1381w, 1277w, 1098s, 1055s, 777w and 754w; *m*/*z* 687 (M − Cl, 100) and 623 (M − Cl − EtCl, 12%); λ_{max}/nm (ε/dm^3 mol^{-1} cm^{-1}) (CH_2Cl_2) 406 (70), 426 (72), 700 (23) and 1100 (37).

[Ni$_2$L^{1}Cl$_2$][BPh$_4$] 3. A solution of $NaBPh_4$ (0.34 g, 1.0 mmol) in ethanol (25 cm^3) was added to a solution of complex **2** (0.72 g, 1.0 mmol) in thf (50 cm^3) and stirred for 3 h at room temperature. After removal of all volatile material under vacuum the residue was taken up in thf and filtered. Evaporation of the solvent afforded the raw product as a green powder (0.90 g, 89%). Vapour diffusion of Et_2O into a solution of the product in thf gave green *crystals* of [Ni$_2$L^{1}Cl$_2$][BPh$_4$] **3** (0.52 g, 52%) (Found: C, 58.45; H, 7.19; N, 8.35. $C_{49}H_{71}BCl_2N_6Ni_2S_2$ requires C, 58.42; H, 7.10; N, 8.34%); $\tilde{\nu}_{max}$/cm^{-1} (KBr) 3053–2928vs, 1578w, 1478s, 1456s, 1315w, 1266w, 1103s, 735vs, 705vs and 611s; *m*/*z* 686 ($L^1Ni_2Cl_2$, 100) and 651 (L^1Ni_2Cl, 12%); λ_{max}/nm (ε/dm^3 mol^{-1} cm^{-1}) (CH_2Cl_2) 405 (120), 678 (45) and 1130 (55).

Crystallography

The measurements were carried out at 200 K on a Siemens P4 (Nicolet Syntex) R3m/v four-circle diffractometer with graphite-monochromated Mo-Kα radiation (λ 0.710 73 Å). All calculations were performed with a micro-vax computer using the SHELXTL PLUS software package.[24] Structures were solved by direct methods with SHELXS 86 and refined with the SHELXL 93 programs.[24] An absorption correction (ψ scan, Δψ = 10°) was applied to all data. Atomic coordinates and anisotropic thermal parameters of the non-hydrogen atoms

were refined by full-matrix least-squares calculation. The hydrogen atoms were placed at calculated positions and allowed to ride on the atoms to which they were attached. Table 5 compiles the data for the structure determinations.

CCDC reference number 186/782.

See http://www.rsc.org/suppdata/dt/1998/199/ for crystallographic files in .cif format.

Acknowledgements

We are grateful to Professor Dr. G. Huttner for his generous and continuous support of our work as well as to the Deutsche Forschungsgemeinschaft (Habilitandenstipendium for F. M.) and the Fonds der Chemischen Industrie.

References

1 K. D. Karlin, *Science*, 1993, **261**, 701; R. H. Holm, *Pure Appl. Chem.*, 1995, **67**, 217; N. Sträter, W. N. Lipscomb, T. Klabunde and B. Krebs, *Angew. Chem.*, 1996, **108**, 2158; *Angew. Chem.*, *Int. Ed. Engl.*, 1996, **35**, 2024.

2 W. Kaim and B. Schwederski, *Bioanorganische Chemie*, Teubner, Stuttgart, 1991.

3 See, for example, S. R. Collinson and D. E. Fenton, *Coord. Chem. Rev.*, 1996, **148**, 19; H. Okawa and H. Sakiyama, *Pure Appl. Chem.*, 1995, **67**, 273; L. Que, jun. and Y. Dong, *Acc. Chem. Res.*, 1996, **29**, 190.

4 (*a*) D. Volkmer, B. Hommerich, K. Griesar, W. Haase and B. Krebs, *Inorg. Chem.*, 1996, **35**, 3792; (*b*) M. Rapta, P. Kamaras and G. B. Jameson, *Polyhedron*, 1996, **15**, 1943; (*c*) D. E. Fenton and H. Okawa, *Chem. Ber./Recueil*, 1997, **130**, 433.

5 J. H. Satcher, jun., M. W. Droege, T. J. R. Weakley and R. T. Taylor, *Inorg. Chem.*, 1995, **34**, 3317.

6 H. Steinhagen and G. Helmchen, *Angew. Chem.*, *Int. Ed. Engl.*, 1996, **35**, 2339.

7 P. J. Steel, *Coord. Chem. Rev.*, 1990, **106**, 227; A. P. Sadimenko and S. S. Basson, *ibid.*, 1996, **147**, 247.

8 T. G. Schenck, J. M. Downes, C. R. C. Milne, P. B. Mackenzie, H. Boucher, J. Whelan and B. Bosnich, *Inorg. Chem.*, 1985, **24**, 2334.

9 (*a*) T. Kamiusuki, H. Okawa, E. Kitaura, M. Koikawa, N. Matsumoto, S. Kida and H. Oshio, *J. Chem. Soc.*, *Dalton Trans.*, 1989, 2077; (*b*) T. Kamiusuki, H. Okawa, N. Matsumoto and S. Kida, *J. Chem. Soc.*, *Dalton Trans.*, 1990, 195; (*c*) T. Kamiusuki, H. Okawa, K. Inoue, N. Matsumoto, M. Kodera and S. Kida, *J. Coord. Chem.*, 1991, **23**, 201; (*d*) M. Itoh, K. Motoda, K. Shindo, T. Kamiusuki, H. Sakiyama, N. Matsumoto and H. Okawa, *J. Chem. Soc.*, *Dalton Trans.*, 1995, 3635.

10 B. Mernari, F. Abraham, M. Lagrenne, M. Drillon and P. Legoll, *J. Chem. Soc.*, *Dalton Trans.*, 1993, 1707.

11 L. Behle, M. Neuburger, M. Zehnder and T. A. Kaden, *Helv. Chim. Acta*, 1995, **78**, 693.

12 J. Pons, X. López, E. Benet, J. Casabó, F. Teixidor and F. J. Sánchez, *Polyhedron*, 1990, **9**, 2835; J. Pons, F. J. Sánchez, A. Labarta, J. Casabó, F. Teixidor and A. Caubet, *Inorg. Chim. Acta*, 1993, **208**, 167.

13 (*a*) F. Meyer, S. Beyreuther, K. Heinze and L. Zsolnai, *Chem. Ber./Recueil*, 1997, **130**, 605; (*b*) F. Meyer, K. Heinze, B. Nuber and L. Zsolnai, *J. Chem. Soc.*, *Dalton Trans.*, following paper; (*c*) F. Meyer, A. Jacobi and L. Zsolnai, *Chem. Ber./Recueil*, 1997, **130**, 1441.

14 See, for example, (*a*) V. P. Hanot, T. D. Robert, J. Kolnaar, J. G. Haasnoot, J. Reedijk, H. Kooijman and A. L. Spek, *J. Chem. Soc.*, *Dalton Trans.*, 1996, 4275; (*b*) P. L. Jones, J. C. Jeffery, J. A. McCleverty and M. D. Ward, *Polyhedron*, 1997, **16**, 1567; (*c*) J. C. Jeffery, P. L. Jones, K. L. V. Mann, E. Psillakis, J. A. McCleverty, M. D. Ward and C. M. White, *Chem. Commun.*, 1997, 175.

15 E. Mugnaini and P. Grünanger, *Atti. Accad. Naz. Lincei*, *Cl. Sci. Fis. Mat. Nat.*, *Rend.*, 1953, **14**, 958.

16 G. Fallani, R. Morassi and F. Zanobini, *Inorg. Chim. Acta*, 1975, **12**, 147; P. Stavropoulos, M. C. Muetterties, M. Carrié and R. H. Holm, *J. Am. Chem. Soc.*, 1991, **113**, 8485.

17 D. Nicholls, in *Comprehensive Inorganic Chemistry*, eds. J. C. Bailar, H. J. Emeléus, Sir R. Nyholm and A. F. Trotman-Dickenson, 1st edn., Pergamon, Oxford, 1973, vol. 3, p. 1152 ff.

18 J. Huheey, E. Keiter and R. Keiter, *Anorganische Chemie*, 2nd edn., Walter de Gruyter, Berlin, 1995, p. 517.

19 M. Ciampolini, N. Nardi and G. P. Speroni, *Coord. Chem. Rev.*, 1966, **1**, 222; C. Furlani, *Coord. Chem. Rev.*, 1968, **3**, 141.

20 C. J. O'Connor, *Prog. Inorg. Chem.*, 1982, **29**, 203.

21 (*a*) V. M. Crawford, M. W. Richardson, J. R. Wasson, D. J. Hodgson and W. E. Hatfield, *Inorg. Chem.*, 1976, **15**, 2107; (*b*) O. Kahn, *Molecular Magnetism*, VCH, Weinheim, 1993.

22 P. Chauduri, H.-J. Küppers, K. Wieghardt, S. Gehring, W. Haase, B. Nuber and J. Weiss, *J. Chem. Soc.*, *Dalton Trans.*, 1988, 1367.

23 K. K. Nanda, R. Das, L. K. Thompson, K. Venkatsubramanian, P. Paul and K. Nag, *Inorg. Chem.*, 1994, **33**, 1188; K. K. Nanda, L. K. Thompson, J. N. Bridson and K. Nag, *J. Chem. Soc.*, *Chem. Commun.*, 1994, 1337.

24 G. M. Sheldrick, SHELXTL PLUS, Program Package for Structure Solution and Refinement, Siemens Analytical Instruments, Madison, WI, 1990; SHELXL 93, Program for Crystal Structure Refinement, Universität Göttingen, 1993; SHELXS 86, Program for Crystal Structure Solution, Universität Göttingen, 1986.

Received 31*st July* 1997; *Paper* 7/05543I